

# Robustness of Majorana edge states of short-length Kitaev chains coupled with environment

Motohiko Ezawa<sup>1</sup>

<sup>1</sup>*Department of Applied Physics, University of Tokyo, Hongo 7-3-1, 113-8656, Japan*

Recently, the two-site Kitaev model hosting Majorana edge states was experimentally realized based on double quantum dots. In this context, we construct two-band effective models describing Majorana edge states of a finite-length Kitaev chain by using the isospectral matrix reduction method. We analytically estimate the robustness of Majorana edge states as a function of model parameters. We also study effects of coupling to an environment based on non-Hermitian Hamiltonians derived from the Lindblad equation. We study three types of dissipation, a local one, an adjacent one and a global one. It is found that the Majorana zero-energy edge states acquire nonzero energy such as  $E \propto \pm (i\gamma)^L$  for the local dissipation, where  $\gamma$  is the magnitude of the dissipation and  $L$  is the length of the chain. On the other hand, the Majorana zero-energy edge states acquire nonzero energy such as  $E \propto \pm i\gamma$  irrespective of the length  $L$  for the global dissipation. Hence, the Majorana edge states are robust against the local dissipation but not against the global one. Our results will be useful for future studies on Majorana edge states based on quantum dots.

## I. INTRODUCTION

Majorana fermions are key for topological quantum computation[1–6]. The Majorana edge states form a nonlocal qubit, which is robust for local perturbation. Thus, the qubit based on Majorana fermions will resolve the problem of decoherence in quantum computation. Majorana fermions are materialized in topological superconductors[7–10]. A simplest model of a topological superconductor hosting Majorana fermions is the Kitaev chain[11]. Despite the simpleness of the model, it is hard to materialize it because it is hard to realize the  $p$ -wave superconducting order on the lattice. Recently, the two-site Kitaev chain was experimentally realized in double quantum dots[12]. In addition, the three-site Kitaev chain was also experimentally realized in a nanowire device[13]. It evokes studies on the Minimal Kitaev chain based on double quantum dots[14–19] and short-length quantum dots[20–22]. However, the Majorana edge states in the two-site Kitaev chain is not topologically protected. Indeed, we need a precise tuning of the model parameters so that the Majorana edge states exist exactly at the zero energy. On the other hand, the Majorana edge states are robust if the length of the Kitaev chain is long enough. It is hard to increase the number of quantum dots in the current technology. There are studies on the condition for the existence of the Majorana edge states to have exact zero energy[23–27]. However, there is no construction of the two-band effective model based on Majorana edge states for a finite-length chain. It is intriguing if we can estimate the robustness of the Majorana edge states for a finite-length Kitaev chain. It is discussed[11] that the robustness of the Majorana zero-energy states increases exponentially as a function of the length of the Kitaev chain.

The platform of the Majorana fermions such as a quantum dot system has an interaction with another system such as a substrate. In general, the coupling to bath makes the system an open quantum system. It is commonly analyzed based on the Lindblad equation[28]. The short-time dynamics is well described by a non-Hermitian Hamiltonian derived from the Lindblad equation[28]. A Kitaev chain with loss and gain is studied in the context of non-Hermitian Hamiltonian[29–37].

In this paper, we construct effective two-band models for

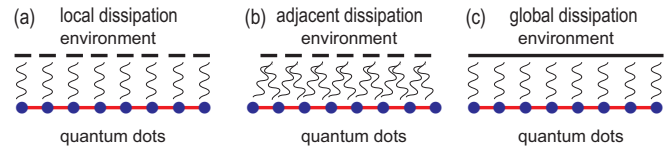


FIG. 1. Illustration of (a) local dissipation, where a quantum dot and an environment interact independently in each single quantum dot, (b) adjacent dissipation, where two quantum dots and an environment interact in nearest-neighbor sites, and (c) global dissipation, where every quantum dots and an environment interact coherently.

the Majorana edge states by using the isospectral matrix reduction method[38, 39]. In addition, we study the effect of the coupling between an environment based on the non-Hermitian Hamiltonian formalism. We study three cases of dissipation. The first one is a local dissipation, where there are hoppings within a single site via an environment as in Fig.1(a). The second one is an adjacent dissipation, where there are hopping between nearest-neighbor sites via an environment as in Fig.1(b). The last one is a global dissipation, where the every site is coherently coupled via an environment as in Fig.1(c). We find that the Majorana edge states are robust against the local dissipation because  $E \propto \pm (i\gamma)^L$  but not against the global dissipation because  $E \propto \pm i\gamma$  irrespective of the length  $L$ , when the amplitude of the dissipation  $\gamma$  is small enough.

## II. KITAEV CHAIN

The Kitaev  $p$ -wave superconductor model is defined on the 1D lattice as[8, 11]

$$\hat{H} = -\mu \sum_{x=1}^{L-1} c_x^\dagger c_x - t \sum_{x=1}^{L-1} (c_x^\dagger c_{x+1} + c_{x+1}^\dagger c_x) - \sum_{x=1}^{L-1} (\Delta c_x c_{x+1} + \Delta c_{x+1}^\dagger c_x^\dagger), \quad (1)$$

where  $\mu$  is the chemical potential,  $t > 0$  is the nearest-neighbor hopping strength,  $\Delta > 0$  is the  $p$ -wave pairing amplitude of the superconductor, and  $L$  is the length of the chain.

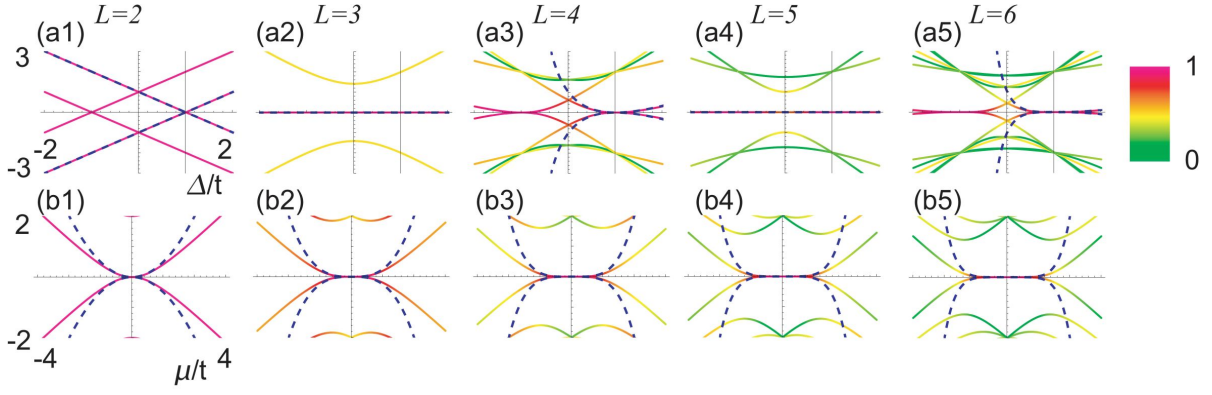


FIG. 2. (a1)~(a4) The energy  $E/t$  as a function of  $\Delta/t$ . We have set  $\mu = 0$ . (b1)~(b4) The energy as a function of  $\mu/t$ . We have set  $\Delta = t$ . Blue dotted curves are the energy derived from the effective two-band model. (a1) and (b1)  $L = 2$ , (a2) and (b2)  $L = 3$ , (a3) and (b3)  $L = 4$ , (a4) and (b4)  $L = 5$  and (a5) and (b5)  $L = 6$ . (c) Color palette indicating the amplitude at the edge sites, where red color indicates the edge states and the green color indicates the bulk states.

### A. Majorana representation

The system is topological for  $|\mu| < 2t$ , where Majorana edge states emerge at both the edges of the chain. We rewrite the fermion operator in terms of two Majorana operators as

$$c_x = \left( \frac{\gamma_{B,x} + i\gamma_{A,x}}{2} \right), \quad c_x^\dagger = \frac{\gamma_{B,x} - i\gamma_{A,x}}{2}, \quad (2)$$

where these Majorana operators satisfy

$$\gamma_{\alpha,x} = \gamma_{\alpha,x}^\dagger, \quad \{\gamma_{\alpha,x}, \gamma_{\alpha',x'}\} = 2\delta_{\alpha\alpha'}\delta_{xx'} \quad (3)$$

with  $\alpha = A, B$ . The Hamiltonian is rewritten in terms of Majorana operators as

$$\begin{aligned} \hat{H} = & -\frac{\mu}{2} \sum_{x=1}^{L-1} (1 + i\gamma_{B,x}\gamma_{A,x}) \\ & - i \sum_{x=1}^{L-1} [(\Delta + t)\gamma_{B,x}\gamma_{A,x+1} + (\Delta - t)\gamma_{A,x}\gamma_{B,x+1}]. \end{aligned} \quad (4)$$

When  $\mu = 0$  and  $t = \Delta \neq 0$ , where the system is topological, the Hamiltonian is simplified as

$$\hat{H} = -2it \sum_{x=1}^{L-1} \gamma_{B,x}\gamma_{A,x+1} = 4t \sum_{x=1}^{L-1} \left( d_x^\dagger d_x - \frac{1}{2} \right), \quad (5)$$

where

$$d_x = \frac{1}{2} (\gamma_{A,x+1} + i\gamma_{B,x}), \quad d_x^\dagger = \frac{1}{2} (\gamma_{A,x+1} - i\gamma_{B,x}). \quad (6)$$

The system is exactly solvable. The ground states are given by  $d_x|0\rangle_d = 0$  with the energy  $-2t$ , whose excited states are  $|1\rangle_d = d_x^\dagger|0\rangle_d$  with the energy  $2t$ . They constitute the bulk band. Apart from them, because this Hamiltonian does not

contain  $\gamma_{A,1}$  and  $\gamma_{B,N}$ , there exist two Majorana states perfectly localized at the two edge sites and exactly at the zero energy. A non-local fermion operator is defined from them as

$$f = \frac{1}{2} (\gamma_{A,1} + i\gamma_{B,N}). \quad (7)$$

A qubit ( $|0\rangle_{\text{qubit}}, |1\rangle_{\text{qubit}}$ ) is constructed such as  $f|0\rangle_{\text{qubit}} = 0$  and  $|1\rangle_{\text{qubit}} = f^\dagger|0\rangle_{\text{qubit}}$ . It is interesting to note that the Majorana chain even with  $L = 2$  is possible to support a qubit.

We show the energy spectrum of (1) as a function of  $\Delta/t$  for  $L = 2, 3, 4, 5, 6$  in Fig.2(a1)~(a5) and that as a function of  $\mu/t$  in Fig.2(b1)~(b5). Especially, the energy has a linear dependence  $E = |\Delta - t|$  for the two-site Kitaev chain with  $\mu = 0$  as shown in Fig.2(a1). On the other hand, the energy has a parabolic dependence  $E \propto \mu^2$  for the two-site Kitaev chain with  $\Delta = t$  as shown in Fig.2(b1).

The real part of the energy is exactly zero for odd length model as shown in Fig.2(a2) and (a4). We will analytically verify these results by deriving an effective two-band model in the following.

### III. OPEN QUANTUM SYSTEM

Effects of the coupling between the system and an environment are described by the Lindblad equation[28] for the density matrix  $\rho$  as

$$\frac{d\rho}{dt} = -\frac{i}{\hbar} [\hat{H}, \rho] + \left( \sum_{\alpha} L_{\alpha}\rho L_{\alpha}^\dagger - \frac{1}{2} \{L_{\alpha}^\dagger L_{\alpha}, \rho\} \right), \quad (8)$$

where  $L$  is the Lindblad operator describing the dissipation. This equation is rewritten in the form of

$$\frac{d\rho}{dt} = -\frac{i}{\hbar} (\hat{H}_{\text{eff}}\rho - \rho\hat{H}_{\text{eff}}^\dagger) + \sum_{\alpha} L_{\alpha}\rho L_{\alpha}^\dagger, \quad (9)$$

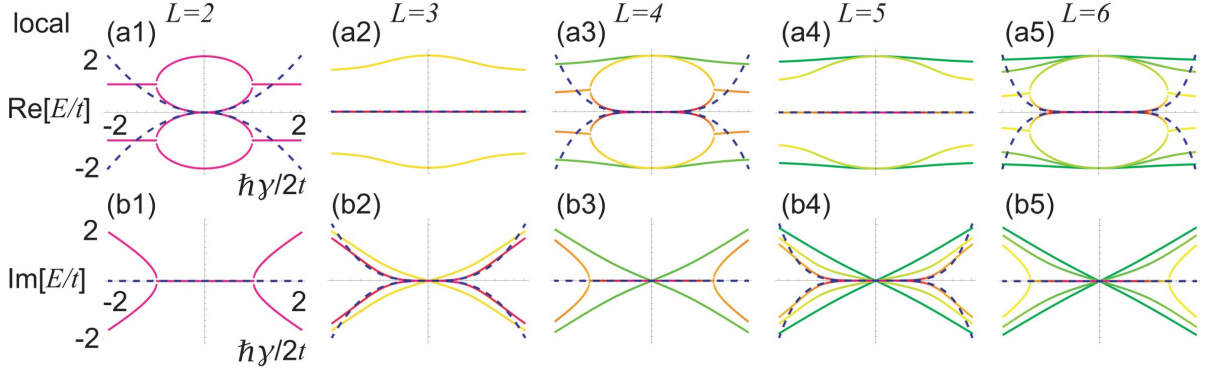


FIG. 3. (a1)~(a4) real part and (b1)~(b4) imaginary part of energy as a function of the local dissipation  $\hbar\gamma/2t$ . (a1) and (b1)  $L = 2$ , (a2) and (b2)  $L = 3$ , (a3) and (b3)  $L = 4$ , (a4) and (b4)  $L = 5$  and (a5) and (b5)  $L = 6$ . We have set  $\Delta = t$  and  $\mu = 0$ . See the color palette in Fig.2.

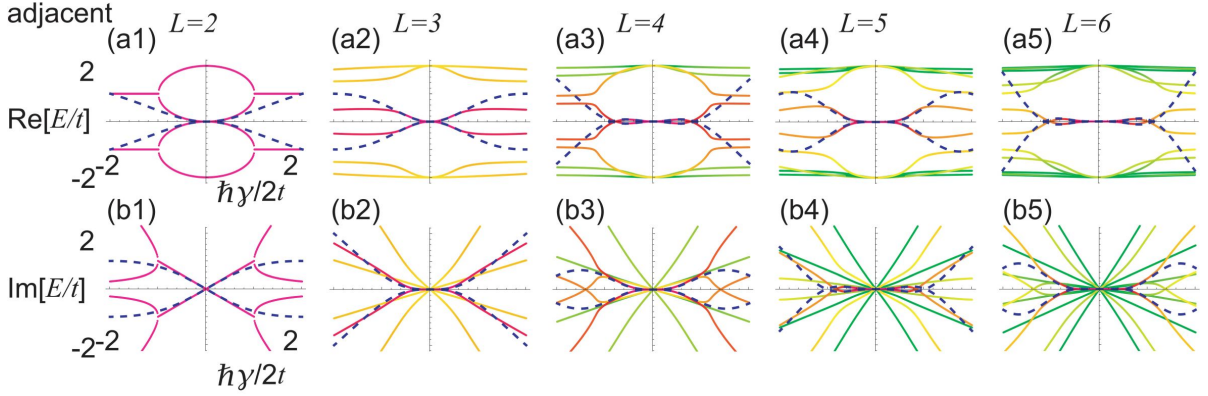


FIG. 4. (a1)~(a4) real part and (b1)~(b4) imaginary part of energy as a function of the adjacent dissipation  $\hbar\gamma/2t$ . The horizontal axis is  $\eta_{\text{adj}}$ . (a1) and (b1)  $L = 2$ , (a2) and (b2)  $L = 3$ , (a3) and (b3)  $L = 4$ , (a4) and (b4)  $L = 5$  and (a5) and (b5)  $L = 6$ . We have set  $\Delta = t$  and  $\mu = 0$ . See the color palette in Fig.2.

where  $H_{\text{eff}}$  is a non-Hermitian effective Hamiltonian defined by  $H_{\text{eff}} \equiv H + H_{\text{dissipation}}$  with the dissipation Hamiltonian

$$\hat{H}_{\text{dissipation}} \equiv -\frac{i\hbar}{2}L^\dagger L. \quad (10)$$

It describes a short-time dynamics[28]. We consider three types of dissipations as illustrated in Fig.1.

### A. Local dissipation

First, we study the local dissipation[37], where the Lindblad operators are given by

$$L_x^- = \sqrt{\gamma_-}c_x, \quad L_x^+ = \sqrt{\gamma_+}c_x^\dagger, \quad (11)$$

where  $\gamma_\pm$  represent the dissipation. They describes the effect that the particle is coming in and out of a single site. The corresponding dissipation Hamiltonian reads

$$\hat{H}_{\text{dissipation}} = -\frac{i\hbar}{2} \sum_{x=1}^L [\gamma_- c_x^\dagger c_x + \gamma_+], \quad (12)$$

where  $\gamma \equiv \gamma_- - \gamma_+$ . By introducing a complex chemical potential

$$\tilde{\mu} = \mu + \frac{i\hbar}{2}\gamma, \quad (13)$$

the effect of the local dissipation is fully taken into account. We show the energy spectrum as a function of  $\gamma$  in Fig.3. The real part of the energy for odd length is exactly zero as shown in Fig.3(a2) and (a4). On the other hand, the imaginary part of the energy for even length is exactly zero if the dissipation is smaller than a certain critical value  $|\gamma| < |\gamma_{\text{critical}}|$ . The flat region of the zero-energy Majorana edge states is expanded for longer chains. We derive these properties based on an effective model with the use of the isospectral matrix reduction method in Sec.V B.

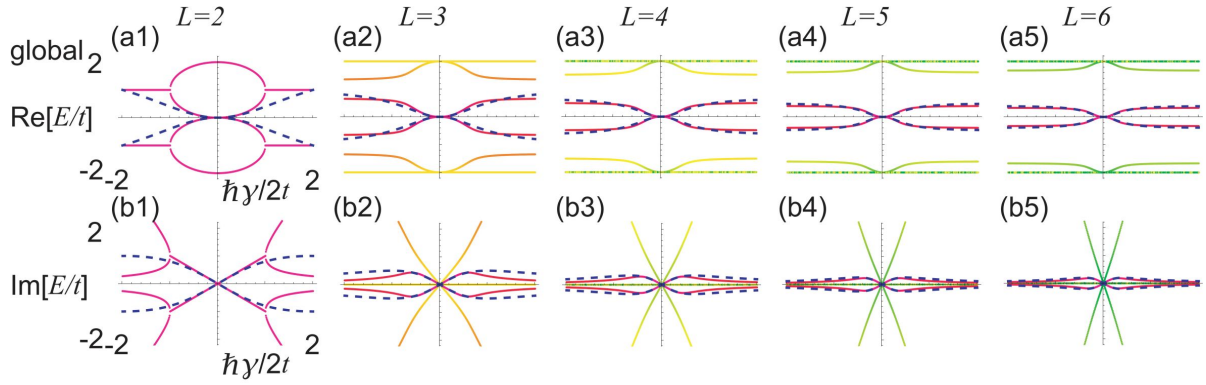


FIG. 5. (a1)~(a4) real part and (b1)~(b4) imaginary part of energy as a function of the global dissipation  $\hbar\gamma/2t$ . The horizontal axis is  $\eta_{\text{global}}$ . (a1) and (b1)  $L = 2$ , (a2) and (b2)  $L = 3$ , (a3) and (b3)  $L = 4$ , (a4) and (b4)  $L = 5$  and (a5) and (b5)  $L = 6$ . We have set  $\Delta = t$  and  $\mu = 0$ . See the color palette in Fig.2.

### B. Adjacent dissipation

Next, we study the adjacent dissipation[40], where the Lindblad operators are given by

$$L_x^- = \sqrt{\gamma_-/2}(c_x + c_{x+1}), \quad L_j^+ = \sqrt{\gamma_+/2}(c_x^\dagger + c_{x+1}^\dagger). \quad (14)$$

They describe the effect that the particle can hop between nearest-neighbor sites via an environment. The corresponding dissipation Hamiltonian reads

$$\begin{aligned} \hat{H}_{\text{dissipation}} &= \frac{\gamma_+}{2} \\ &= -\frac{i\hbar}{2} \sum_{x=1}^{L-1} \frac{\gamma}{2} \left( c_x^\dagger c_x + c_x^\dagger c_{x+1} + c_{x+1}^\dagger c_x + c_{x+1}^\dagger c_{x+1} \right). \end{aligned} \quad (15)$$

The effect of the adjacent dissipation is taken into account by considering the complex chemical potential and the complex hopping defined by

$$\tilde{\mu} = \mu + \frac{i\hbar}{2}\gamma, \quad \tilde{t} = t + \frac{i\hbar}{2}\gamma. \quad (16)$$

We show the energy spectrum as a function of  $\gamma$  in Fig.4. The imaginary part of the energy acquire nonzero energy as a linear function of  $\gamma$  for  $L = 2$  as shown in Fig.4(b1). This is because the two Majorana edge states couple directly via the adjacent dissipation term. It follows from Fig.4 that deviations from the zero energy of the Majorana edge states becomes smaller for longer chains. Comparing Figs.3 and 4, the Majorana edge states are found to be more fragile than the local dissipation. We derive these properties based on an effective model with the use of the isospectral matrix reduction method in Sec.V C.

### C. Global dissipation

Finally, we study the global dissipation, where the Lindblad operators are given by

$$L_x^- = \sqrt{\gamma_-} \sum_{x=1}^L c_x, \quad L_x^+ = \sqrt{\gamma_+} \sum_{x=1}^L c_x^\dagger. \quad (17)$$

They describe the effect that all particles are equally coupled via an environment. The corresponding dissipation Hamiltonian reads

$$\begin{aligned} \hat{H}_{\text{dissipation}} &= -\frac{i\hbar}{2}\gamma \sum_{x,x'=1}^L \left( c_x^\dagger c_x + c_x^\dagger c_{x'} + c_{x'}^\dagger c_x + c_{x'}^\dagger c_{x'} \right) \\ &\quad + \gamma_+, \end{aligned} \quad (18)$$

which is highly nonlocal. We show the energy spectrum as a function of  $\gamma$  in Fig.5 for  $L = 2, 3, 4, 5$ . It is found from Fig.5(b1)~(b5) that the imaginary part of the energy is linear as a function of  $\gamma$  irrespective of the length of the chain although the slope becomes smaller for a longer chain. Hence, the Majorana edge states are not robust in the presence of the global dissipation even for a long Kitaev chain. It is natural because the global dissipation term couples the Majorana edge states directly. We derive these properties based on an effective model with the use of the isospectral matrix reduction method in Sec.V D.

## IV. MINIMAL KITAEV CHAIN

In the presence of the local dissipation or the adjacent dissipation, the Hamiltonian of the two-site Kitaev chain reads

$$\hat{H} = \begin{pmatrix} c_1^\dagger & c_2^\dagger & c_1 & c_2 \end{pmatrix} H \begin{pmatrix} c_1 \\ c_2 \\ c_1^\dagger \\ c_2^\dagger \end{pmatrix}, \quad (19)$$

with

$$H = \begin{pmatrix} -\tilde{\mu} & -\tilde{t} & 0 & \Delta \\ -\tilde{t} & -\tilde{\mu} & -\Delta & 0 \\ 0 & -\Delta & \tilde{\mu} & \tilde{t} \\ \Delta & 0 & \tilde{t} & \tilde{\mu} \end{pmatrix} \quad (20)$$

where we use the complex chemical potential  $\tilde{\mu}$  in (13) for the local dissipation and the complex chemical potential  $\tilde{\mu}$  and the complex hopping  $\tilde{t}$  in (16) for the adjacent dissipation. The energy spectrum is exactly obtained as

$$E = \pm \tilde{t} \pm \sqrt{\Delta^2 + \tilde{\mu}^2}. \quad (21)$$

We note that the adjacent dissipation and the global dissipation is identical for  $L = 2$ .

## V. ISOSPECTRAL MATRIX REDUCTION METHOD

It is impossible to exactly diagonalize the Hamiltonian matrix hosting Majorana edge states except for the exactly solvable parameter  $\mu = 0$ ,  $\Delta = \pm t$  for the Kitaev chain for  $L \geq 3$ .

We derive an effective two-band model near the zero-energy describing the Majorana edge states based on the isospectral matrix reduction method[38, 39]. We first diagonalize the Hamiltonian matrix for  $\mu = 0$ ,  $\Delta = t$  as

$$\begin{aligned} H' &\equiv U H U^{-1} \\ &= \text{diag.} \{0, 0, -2t, -2t, \dots, -2t, 2t, 2t, \dots, 2t\} \end{aligned} \quad (22)$$

The first two zero-energy states correspond to the Majorana edge states. Then we divide  $H'$  into the form of

$$H' = \begin{pmatrix} H_1 & V \\ V^\dagger & H_2 \end{pmatrix}, \quad (23)$$

where  $H_1$  is the  $2 \times 2$  matrix and  $H_2$  is the  $(2L-2) \times (2L-2)$  matrix. The eigenequation reads

$$\begin{pmatrix} H_1 & V \\ V^\dagger & H_2 \end{pmatrix} \begin{pmatrix} \psi_1 \\ \psi_2 \end{pmatrix} = E \begin{pmatrix} \psi_1 \\ \psi_2 \end{pmatrix}, \quad (24)$$

from which we derive

$$\psi_2 = (E - H_2)^{-1} V^\dagger \psi_1. \quad (25)$$

Then, we obtain a single nonlinear eigen equation for  $\psi_1$  as

$$\tilde{H}(E) \psi_1 = E \psi_1, \quad (26)$$

where

$$\tilde{H}(E) = H_1 + V (E - H_2)^{-1} V^\dagger. \quad (27)$$

Exact solutions may be obtained by solving the nonlinear equation. However, it is practically impossible to solve it because it is an algebraic equation of the order of  $E^{2L}$ . Instead, we seek a solution in the vicinity of the zero energy, where the Hamiltonian is well approximated by

$$H_{\text{eff}} \equiv H_1 - V H_2^{-1} V^\dagger. \quad (28)$$

The second term is written in the form of

$$-V H_2^{-1} V^\dagger = F \sigma_x. \quad (29)$$

We explicitly determine  $H_{\text{eff}}$  in what follows.

## A. Hermitian model

First, we derive an effective two-band model for the Hermitian system. We find

$$H_1 = (t - \Delta) \sigma_x \quad (30)$$

for  $L = 2$  and  $H_1 = 0$  for  $L \geq 3$ . On the other hand, we find

$$F = \frac{1}{(\Delta + t)^{L-1}} \sum_{m=0}^{\lfloor L/2 \rfloor} \binom{L-m}{m} \mu^{L-2m} (\Delta^2 - t^2)^{2m} \quad (31)$$

for  $L \geq 2$ . The energy is given by

$$E = \pm F. \quad (32)$$

If  $\mu = 0$ , we have  $F = 0$  for odd  $L$ , which well describes the energy near the zero energy as shown in Fig.2(a2) and (a4). On the other hand, we find

$$F = -\frac{(\Delta - t)^{L/2}}{(\Delta + t)^{L/2+1}} \propto (\Delta - t)^{L/2} \quad (33)$$

for even  $L$ , which well describes the energy near the zero energy as shown in Fig.2(a1), (a3) and (a5). It is almost zero for small  $|\Delta - t|$  and large  $L$ , where the Majorana edge states are robust.

If  $\Delta = t$ , we have

$$F = -\frac{\mu^L}{(2t)^{L-1}} \propto \mu^L. \quad (34)$$

It well fits the energy near the zero energy as shown in Fig.2(b1)~(b5). It is almost zero for small  $\mu$  and large  $L$ , where the Majorana edge states are robust.

## B. Local dissipation

Next, we derive effective two-band models for the local dissipation with  $\Delta = t$  and  $\mu = 0$ . We find

$$H_{\text{eff}} = -\frac{(i\gamma)^L}{(2t)^{L-1}} \quad (35)$$

for  $L \geq 2$ . This formula well explains the fact that the real [imaginary] part of the energy is zero for even [odd]  $L$  as shown in Fig.3(a2) and (a4), [(b1) and (b3)]. Hence the Majorana edge states becomes robust for a long chain.

## C. Adjacent dissipation

We derive effective two-band models for the adjacent dissipation with  $\mu = 0$ . We find

$$H_1 = (t + i\gamma - \Delta) \sigma_x \quad (36)$$

for  $L = 2$  and  $H_1 = 0$  for  $L \geq 3$ . On the other hand,

$$F = - \sum_{m=0}^{\lfloor L/2 \rfloor} \binom{L-m}{m} \frac{(i\gamma)^{L-2m}}{(\Delta+t)^{L-1}} \left( \Delta^2 - (t+i\gamma)^2 \right)^m \quad (37)$$

for  $L \geq 2$ . For small  $\gamma$  ( $|\gamma/t| \ll 1$ ), they are explicitly given by

$$\begin{aligned} F &= -i\gamma - \gamma^2/2t + \dots & \text{for } L = 2, \\ F &= -3i\gamma^3/4t^2 + \gamma^2/2t + \dots & \text{for } L = 3, \\ F &= -i\gamma^3/t^2 - \gamma^2/2t + \dots & \text{for } L = 4, \\ F &= -i\gamma^3/4t^2 - \gamma^4/4t^3 + \dots & \text{for } L = 5, \\ F &= i\gamma^3/4t^2 + \gamma^4/t^3 + \dots & \text{for } L = 6, \end{aligned} \quad (38)$$

In general,

$$F = ia\gamma^A + b\gamma^B + \dots, \quad (39)$$

with certain real numbers  $a$  and  $b$ , where

$$A = 2 \left\lfloor \frac{L+1}{4} \right\rfloor + 1, \quad B = 2 \left\lfloor \frac{L-1}{4} \right\rfloor + 2. \quad (40)$$

The robustness of the Majorana edge modes is enhanced when the chain length becomes longer. However, it is more fragile than the local dissipation.

#### D. Global dissipation

Finally, we derive effective two-band models for the global dissipation with  $\Delta = t$  and  $\mu = 0$ . We find

$$H_1 = i\gamma\sigma_x, \quad F = \frac{(L-1)\gamma^2}{2t + i(L-1)\gamma} \sigma_x \quad (41)$$

for  $L \geq 2$ . For small  $\gamma$  ( $|\gamma/t| \ll 1$ ), the Hamiltonian is approximated as

$$H_{\text{eff}} \simeq \left( i\gamma + \frac{(L-1)\gamma^2}{2t} \right) \sigma_x. \quad (42)$$

The real part of the energy is parabolic as a function of  $\gamma$  irrespective of the length  $L$  as shown in Fig.5(a1)~(a5), while the imaginary part of the energy is linear as a function of  $\gamma$  irrespective of the length  $L$  as shown in Fig.5(b1)~(b5). Hence, the robustness of the Majorana edge states is not enhanced even if we use a chain with long length  $L$  in the presence of the global dissipation.

Actually, the energy spectrum in the vicinity of the zero energy is exactly obtained without using the isospectral matrix reduction method at the point  $\mu = 0$  and  $\Delta = t$ , whose results reads

$$F = i\frac{L}{2}\gamma + 2t + i\sqrt{\left(\frac{L}{2}\gamma\right)^2 - 2i(L-2)t\gamma - 4t^2}. \quad (43)$$

It gives the same result as in (42) for small  $\gamma$  ( $|\gamma/t| \ll 1$ ).

## VI. DISCUSSION

We have constructed two-band effective models describing the Majorana edge states in the presence of three types of dissipation. We have found the even-odd effect on the stability of the Majorana edge states. We have also found that the robustness of the Majorana edge states is affected by the type of dissipation, where the global dissipation is detrimental to the stability of the Majorana edge states. The local dissipation may be realized when the system couples with the substrate where the real coordinate is a good quantum number. On the other hand, the global dissipation may be realized when the system couples with the substrate where the momentum coordinate is a good quantum number. Our results will be useful for experimental realization of the Kitaev chain based on quantum dots.

This work is supported by CREST, JST (Grants No. JP-MJCR20T2) and Grants-in-Aid for Scientific Research from MEXT KAKENHI (Grant No. 23H00171).

- 
- [1] S. B. Bravyi and A. Yu. Kitaev, Fermionic Quantum Computation, *Annals of Physics* 298, 210 (2002)
  - [2] D. A. Ivanov, Non-Abelian statistics of half-quantum vortices in p-wave superconductors, *Phys. Rev. Lett.* 86, 268 (2001).
  - [3] A. Kitaev, Fault-tolerant quantum computation by anyons, *Ann. Phys.* 303, 2 (2003).
  - [4] S. Das Sarma, M. Freedman, and C. Nayak, Topologically protected qubits from a possible non-Abelian fractional quantum Hall state, *Phys. Rev. Lett.* 94, 166802 (2005).
  - [5] C. Nayak, S. H. Simon, A. Stern, M. Freedman, and S. Das Sarma, Non-Abelian anyons and topological quantum computation, *Rev. Mod. Phys.* 80, 1083 (2008).
  - [6] Motohiko Ezawa, Systematic construction of topological-nontopological hybrid universal quantum gates based on many-body Majorana fermion interactions arXiv:2304.06260
  - [7] X.-L. Qi, S.-C. Zhang, Topological insulators and superconductors, *Rev. Mod. Phys.* 83, 1057 (2011).
  - [8] J. Alicea, New directions in the pursuit of Majorana fermions in solid state systems, *Rep. Prog. Phys.* 75, 076501 (2012)
  - [9] M. Sato and Y. Ando, Topological superconductors: a review, *Rep. Prog. Phys.* 80, 076501 (2017).
  - [10] J. Alicea, Y. Oreg, G. Refael, F. von Oppen and M.P.A. Fisher, Non-Abelian statistics and topological quantum information processing in 1D wire networks, *Nat. Phys.* 7, 412 (2011).
  - [11] A. Yu Kitaev, Unpaired Majorana fermions in quantum wires *Phys.-Usp.* 44 131 (2001)
  - [12] Tom Dvir, Guanzhong Wang, Nick van Loo, Chun-Xiao Liu, Grzegorz P. Mazur, Alberto Bordin, Sebastiaan L. D. ten Haaf,

- Ji-Yin Wang, David van Driel, Francesco Zatelli, Xiang Li, Filip K. Malinowski, Sasa Gazibegovic, Ghada Badawy, Erik P. A. M. Bakkers, Michael Wimmer and Leo P. Kouwenhoven, Realization of a minimal Kitaev chain in coupled quantum dots, *Nature* 614, 445 (2023)
- [13] Alberto Bordin, Xiang Li, David van Driel, Jan Cornelis Wolff, Qingzhen Wang, Crossed Andreev reflection and elastic co-tunneling in a three-site Kitaev chain nanowire device, arXiv:2306.07696
- [14] Athanasios Tsintzis, Ruben Seoane Souto and Martin Leijnse, Creating and detecting poor man's Majorana bound states in interacting quantum dots *Phys. Rev. B* 106, L201404 (2022)
- [15] Chun-Xiao Liu, Haining Pan, F. Setiawan, Michael Wimmer and Jay D. Sau, Fusion protocol for Majorana modes in coupled quantum dots *Phys. Rev. B* 108, 085437 (2023)
- [16] Rouven Koch, David van Driel, Alberto Bordin, Jose L. Lado and Eliska Greplova, Adversarial Hamiltonian learning of quantum dots in a minimal Kitaev chain, arXiv:2304.10852
- [17] Athanasios Tsintzis, Ruben Seoane Souto, Karsten Flensberg, Jeroen Danon and Martin Leijnse, Roadmap towards Majorana qubits and nonabelian physics in quantum dot-based minimal Kitaev chains, arXiv:2306.16289
- [18] D. Michel Pino, Ruben Seoane Souto and Ramon Aguado, Minimal Kitaev–transmon qubit based on double quantum dots, arXiv:2309.12313
- [19] William Samuelson, Viktor Svensson and Martin Leijnse, A minimal quantum dot-based Kitaev chain with only local superconducting proximity effect, arXiv:2310.03536
- [20] Mahan Mohseni, Hassan Allami, Daniel Miravet, David J. Gayowsky, Marek Korkusinski, Pawel Hawrylak, Majorana excitons in a Kitaev chain of semiconductor quantum dots in a nanowire, arXiv:2307.00100
- [21] Ruben Seoane Souto, Athanasios Tsintzis, Martin Leijnse and Jeroen Danon, Probing Majorana localization in minimal Kitaev chains through a quantum dot, arXiv:2308.14751
- [22] Sebastian Miles, David van Driel, Michael Wimmer and Chun-Xiao Liu, Kitaev chain in an alternating quantum dot-Andreev bound state array, arXiv:2309.15777
- [23] Hsien-chung Kao, *Phys. Rev. B* 90, 245435, Chiral zero modes in superconducting nanowires with Dresselhaus spin-orbit coupling, *Phys. Rev. B* 90, 245435 (2014)
- [24] Suraj Hegde, Vasudha Shivamoggi, Smitha Vishveshwara and Diptiman Sen, Quench dynamics and parity blocking in Majorana wires *New J. Phys.* 17 053036 (2015)
- [25] A. A. Zvyagin, Majorana bound states in the finite-length chain *Low Temp. Phys.* 41 625 (2015)
- [26] Chuanchang Zeng, Christopher Moore, Apparao M. Rao, Tudor D. Stanescu, and Sumanta Tewari, Analytical solution of the finite-length Kitaev chain coupled to a quantum dot *Phys. Rev. B* 99, 094523 (2019)
- [27] Nico Leumer, Magdalena Marganska, Bhaskaran Muralidharan and Milena Grifoni, Exact eigenvectors and eigenvalues of the finite Kitaev chain and its topological properties *J. Phys.: Condens. Matter* 32 445502 (2020)
- [28] G. Lindblad, On the generators of quantum dynamical semi-groups, *Commun. Math. Phys.* 48, 119 (1976)
- [29] C. Yuce, Majorana edge modes with gain and loss, *Phys. Rev. A* 93, 062130 (2016)
- [30] Qi-Bo Zeng, Baogang Zhu, Shu Chen, L. You, and Rong Lu, *Phys. Rev. A* 94, 022119 (2016)
- [31] Kohei Kawabata, Yuto Ashida, Hosho Katsura, Masahito Ueda, Parity-time-symmetric topological superconductor, *Phys. Rev. B* 98, 085116 (2018)
- [32] Kohei Kawabata, Sho Higashikawa, Zongping Gong, Yuto Ashida and Masahito Ueda, Topological unification of time-reversal and particle-hole symmetries in non-Hermitian physics *Nat. Com.* 10, 297 (2019)
- [33] Kohei Kawabata, Ken Shiozaki, Masahito Ueda and Masatoshi Sato, Symmetry and Topology in Non-Hermitian Physics, *Phys. Rev. X* 9, 041015 (2019)
- [34] Naoyuki Shibata and Hosho Katsura, Dissipative spin chain as a non-Hermitian Kitaev ladder, *Phys. Rev. B* 99, 174303 (2019)
- [35] Motohiko Ezawa, Braiding of Majorana-like corner states in electric circuits and its non-Hermitian generalization, *Phys. Rev. B* 100, 045407 (2019)
- [36] Xiao-Ming Zhao, Cui-Xian Guo, Su-Peng Kou, Lin Zhuang, and Wu-Ming Liu *Phys. Rev. B* 104, 205131, Defective Majorana zero modes in a non-Hermitian Kitaev chain (2021)
- [37] Simon Lieu, Non-Hermitian Majorana modes protect degenerate steady states, *Phys. Rev. B* 100, 085110 (2019)
- [38] Lumen Eek, Anouar Moustaj, Malte Rontgen, Vincent Pagneux, Vassos Achilleos, and Cristiane Morais Smith, Emergent non-Hermitian models, arXiv:2310.11988
- [39] Malte Rontgen, Xuelong Chen, Wenlong Gao, Maxim Pyzh, Peter Schmelcher, Vincent Pagneux, Vassos Achilleos and Antonin Coutant, Latent Su–Schrieffer–Heeger models, arXiv:2310.07619
- [40] Sebastian Diehl, Enrique Rico, Mikhail A. Baranov and Peter Zoller, Topology by dissipation in atomic quantum wires, *Nature Physics* 7, 971 (2011)